



IL-26 Confers Proinflammatory Properties to Extracellular DNA

Caroline Poli, Jean-François Augusto, Jonathan Dauvé, Clément Adam, Laurence Preisser, Vincent Larochette, Pascale Pignon, Ariel Savina, Simon J. Blanchard, Jean-François Subra, et al.

► To cite this version:

Caroline Poli, Jean-François Augusto, Jonathan Dauvé, Clément Adam, Laurence Preisser, et al.. IL-26 Confers Proinflammatory Properties to Extracellular DNA . Journal of Immunology, 2017, 198 (9), pp.3650-3661. 10.4049/jimmunol.1600594 . inserm-01514382


HAL Id: inserm-01514382

<https://inserm.hal.science/inserm-01514382>


Submitted on 26 Apr 2017

HAL is a multi-disciplinary open access archive for the deposit and dissemination of scientific research documents, whether they are published or not. The documents may come from teaching and research institutions in France or abroad, or from public or private research centers.

L'archive ouverte pluridisciplinaire **HAL**, est destinée au dépôt et à la diffusion de documents scientifiques de niveau recherche, publiés ou non, émanant des établissements d'enseignement et de recherche français ou étrangers, des laboratoires publics ou privés.





ARE YOU A
**SCIENTIFIC
REBEL?**



Unleash your true potential
with the new **CytoFLEX LX**
Flow Cytometer

DARE TO EXPLORE



This information is current as
of April 24, 2017.

IL-26 Confers Proinflammatory Properties to Extracellular DNA

Caroline Poli, Jean François Augusto, Jonathan Dauvé, Clément Adam, Laurence Preisser, Vincent Larochette, Pascale Pignon, Ariel Savina, Simon Blanchard, Jean François Subra, Alain Chevailler, Vincent Procaccio, Anne Croué, Christophe Créminon, Alain Morel, Yves Delneste, Helmut Fickenscher and Pascale Jeannin

J Immunol 2017; 198:3650-3661; Prepublished online 29 March 2017;

doi: 10.4049/jimmunol.1600594

<http://www.jimmunol.org/content/198/9/3650>

Supplementary Material <http://www.jimmunol.org/content/suppl/2017/03/29/jimmunol.1600594.DCSupplemental>

References This article **cites 69 articles**, 27 of which you can access for free at:
<http://www.jimmunol.org/content/198/9/3650.full#ref-list-1>

Subscription Information about subscribing to *The Journal of Immunology* is online at:
<http://jimmunol.org/subscription>

Permissions Submit copyright permission requests at:
<http://www.aai.org/About/Publications/JI/copyright.html>

Email Alerts Receive free email-alerts when new articles cite this article. Sign up at:
<http://jimmunol.org/alerts>



IL-26 Confers Proinflammatory Properties to Extracellular DNA

Caroline Poli,^{*,†,1} Jean François Augusto,^{*,‡,1} Jonathan Dauvé,[§] Clément Adam,^{*} Laurence Preisser,^{*} Vincent Larochette,^{*} Pascale Pignon,^{*} Ariel Savina,[¶] Simon Blanchard,^{*,†} Jean François Subra,^{*,‡} Alain Chevailler,^{*,†} Vincent Procaccio,^{||,#} Anne Croué,^{**} Christophe Créminon,^{††} Alain Morel,^{*,§} Yves Delneste,^{*,†,2} Helmut Fickenscher,^{‡‡,2} and Pascale Jeannin^{*,†,2}

In physiological conditions, self-DNA released by dying cells is not detected by intracellular DNA sensors. In chronic inflammatory disorders, unabated inflammation has been associated with a break in innate immune tolerance to self-DNA. However, extracellular DNA has to complex with DNA-binding molecules to gain access to intracellular DNA sensors. IL-26 is a member of the IL-10 cytokine family, overexpressed in numerous chronic inflammatory diseases, in which biological activity remains unclear. We demonstrate in this study that IL-26 binds to genomic DNA, mitochondrial DNA, and neutrophil extracellular traps, and shuttles them in the cytosol of human myeloid cells. As a consequence, IL-26 allows extracellular DNA to trigger proinflammatory cytokine secretion by monocytes, in a STING- and inflammasome-dependent manner. Supporting these biological properties, IL-10-based modeling predicts two DNA-binding domains, two amphipathic helices, and an in-plane membrane anchor in IL-26, which are structural features of cationic amphipathic cell-penetrating peptides. In line with these properties, patients with active autoantibody-associated vasculitis, a chronic relapsing autoimmune inflammatory disease associated with extensive cell death, exhibit high levels of both circulating IL-26 and IL-26–DNA complexes. Moreover, in patients with crescentic glomerulonephritis, IL-26 is expressed by renal arterial smooth muscle cells and deposits in necrotizing lesions. Accordingly, human primary smooth cells secrete IL-26 in response to proinflammatory cytokines. In conclusion, IL-26 is a unique cationic protein more similar to a soluble pattern recognition receptor than to conventional cytokines. IL-26 expressed in inflammatory lesions confers proinflammatory properties to DNA released by dying cells, setting up a positive amplification loop between extensive cell death and unabated inflammation. *The Journal of Immunology*, 2017, 198: 3650–3661.

Nucleic acids, and especially DNA, constitute potent microbial moieties that activate innate immune cells. Their recognition by DNA sensors, such as TLR9 and stimulator of IFN genes (STING), which are sequestered in endosomes and cytosol, respectively, triggers type I IFN and proinflammatory cytokine secretion, thereby controlling host defense countermeasures (1). Mainly expressed by B lymphocytes and plasmacytoid dendritic cells (pDCs) in humans, TLR9 recognizes DNA containing unmethylated CpG motifs that are more prevalent in microbes (1). STING, expressed in numerous cell types (including myeloid and lymphoid cells) (2, 3), recognizes a wide variety of DNA (4). In physiological conditions, the localization of self-DNA in nucleus and mitochondria avoids its recognition by DNA

sensors. Extracellular and intracellular DNases, which rapidly degrade DNA released by dying cells (5) and aberrant self-DNA present in cytosol and endosomes (6, 7), respectively, also contribute to prevent cell activation by self-DNA.

In pathological conditions such as systemic lupus erythematosus (SLE), chronic polyarthritis, and psoriasis, DNA sensor activation results in chronic inflammation and a type I IFN signature (8, 9). The in vivo break of innate immune tolerance to self-DNA observed in these pathologies has been associated to excessive cell death and defects in dying cell clearance or in DNase activity (10, 11).

However, by itself, the accumulation of extracellular self-DNA could be not sufficient to trigger inflammation. Indeed, large amounts of extracellular DNA fail to stimulate immune cells, both

*CRCINA, INSERM, Université de Nantes, Université d'Angers, LabEx IGO, 49000 Angers, France; [†]Laboratoire d'Immunologie et Allergologie, CHU Angers, 49000 Angers, France; [‡]Service de Néphrologie-Dialyse-Transplantation, CHU Angers, 49000 Angers, France; [§]Institut de Cancérologie de l'Ouest Paul Papin, 49000 Angers, France; [¶]Roche SAS Scientific Partnerships, 92100 Boulogne Billancourt, France; ^{||}INSERM, CNRS, Université d'Angers, 49000 Angers, France; [#]Laboratoire de Biochimie et Génétique, CHU Angers, 49000 Angers, France; ^{**}Laboratoire d'Histopathologie-Cytopathologie, Département de Pathologie Cellulaire et Tissulaire, CHU Angers, 49000 Angers, France; ^{††}Service de Pharmacologie et d'Immunoanalyse, Commissariat à l'Energie Atomique Saclay, iBiTec-S, 91190 Gif sur Yvette, France; and ^{‡‡}Institute for Infection Medicine, Christian Albrecht University of Kiel and University Medical Center Schleswig-Holstein, 24000 Kiel, Germany

¹C.P. and J.F.A. contributed equally to this work.

²Y.D., H.F., and P.J. equivalently supervised this study.

ORCIDs: 0000-0003-1170-5586 (C.P.); 0000-0003-1498-2132 (J.F.A.); 0000-0002-2565-8066 (J.D.).

Received for publication April 4, 2016. Accepted for publication February 24, 2017.

This work was supported by institutional grants from INSERM and the University of Angers and by a grant from Roche SAS (France). The funders had no role in study design, data collection and analysis, decision to publish, or preparation of the manuscript.

Address correspondence and reprint requests to Prof. Pascale Jeannin, CHU Angers, UMR INSERM 1232, Bâtiment IRIS, 4 rue Larrey, F-49933 Angers, France. E-mail address: pascale.jeannin@univ-angers.fr

The online version of this article contains supplemental material.

Abbreviations used in this article: AAV, anti-neutrophil cytoplasmic Ab-associated vasculitis; APBS, Adaptive Poisson-Boltzmann Solver; BVAS, Birmingham vasculitis activity score 2003; CPP, cell-penetrating peptide; IPM, in-plane membrane; ISG, IFN-stimulated gene; mtDNA, mitochondrial DNA; NET, neutrophil extracellular trap; pDC, plasmacytoid dendritic cell; siRNA, short interfering RNA; SLE, systemic lupus erythematosus; SMC, smooth muscle cell; STING, stimulator of IFN gene.

Copyright © 2017 by The American Association of Immunologists, Inc. 0022-1767/17/\$30.00

in vitro (12–14) and in vivo (15). Neutrophil extracellular traps (NETs), which result from the ejection of chromatin into the extracellular space, do not promote inflammation in vivo (16). In support, cargo molecules, allowing extracellular DNA to gain access to intracellular DNA sensors, have been brought out in patients with SLE and psoriasis. In SLE, autoantibodies against nuclear Ags form immune complexes that favor DNA internalization via FcγR and induce type I IFN secretion by pDCs (17). HMGB1 and the cationic amphipathic antimicrobial peptide LL37 facilitate the uptake of NETs by pDCs (18). In psoriasis, LL37, secreted by activated keratinocytes, forms complexes with extracellular DNA and promotes TLR9-dependent pDCs and STING-dependent myeloid cell activation (13, 14). It is likely that still unidentified DNA cargo molecules exist in other sterile inflammatory disorders. Their identification will provide new insights in the physiopathology of chronic inflammatory diseases.

IL-26 is a member of the IL-10–related cytokine subfamily that includes IL-10, IL-19, IL-20, IL-22, and IL-24. The amino acid identity between these cytokines is up to ~30%, whereby characteristic amino acid positions are conserved (19). Accordingly, despite the relatively low sequence identity, all members show a strikingly similar secondary structure, with six or seven α helices and connecting loops (20).

The IL-26 protein contains numerous positively charged amino acids, including 30 residues that are either lysine or arginine (21). Consequently, IL-26 has an isoelectric point of 10.4. IL-26 mRNA has been reported in activated T cells, mainly Th17 cells, and in activated NK cells (21, 22). Patients suffering from chronic inflammatory disorders (Crohn's disease, rheumatoid arthritis, and chronic hepatitis C virus infection) exhibit high levels of seric IL-26, and the presence of IL-26 has been reported in inflammatory and destructive lesions (23–25).

To date, the biological roles of IL-26 and the identification of the IL-26–induced signaling pathways remain unclear. A recent study has reported that IL-26 interacts with DNA, leading to IFN- α secretion by pDCs through TLR9 (26). Initially, IL-26 was reported to induce IL-8 and/or IL-10 by some human epithelial cell lines through a receptor composed of IL-20R1 and IL-10R2 (24, 27, 28). IL-26 also triggers proinflammatory cytokine production by human myeloid cells and NK cells, in the absence of IL-20R1, suggesting that IL-26 is not a classical cytokine (23, 25, 29, 30).

Because IL-26 is overexpressed in chronic sterile inflammatory disorders, we investigated whether IL-26 may render monocytes and neutrophils, which are major contributors to chronic inflammation (31, 32), able to sense extracellular self-DNA. We analyzed the expression and role of IL-26 in anti-neutrophil cytoplasmic Ab–associated vasculitis (AAV), a chronic relapsing–remitting autoimmune disease associated with deleterious inflammation and massive local cell death in injured small vessels.

Materials and Methods

Patients

Sera from 69 AAV patients were collected before the initiation of immunosuppressive treatment, and it was stored in the immunology laboratories of the University Hospital of Angers (France), Le Mans General Hospital (France), and the National Reference center for necrotizing vasculitis and systemic sclerosis (Cochin University Hospital, Paris, France). Biological and clinical characteristics of AAV patients are summarized in Supplemental Table I. The protocol was in agreement with the local ethics committee (2011-06), and blood samples were collected after informed consent of patients was obtained. For 10 patients with active AAV, a second serum was available 6–12 mo after treatment initiation. Disease activity was determined using the Birmingham vasculitis activity score (BVAS) according to the European League Against Rheumatism recommendations (33, 34). Sera from 85 healthy donors were from the blood collection center of Angers (Angers, France; agreement ANG-2003-02).

Recombinant human cytokines

His₆-tagged human IL-26 was expressed in *Escherichia coli* and purified as previously described (35). IL-26 did not contain detectable levels of endotoxin (23), and SDS-PAGE silver staining confirmed the absence of protein contaminants (Supplemental Fig. 1). IL-10, IL-22, IL-24, and IL-29 were purchased from ImmunoTools (Friesoythe, Germany), and IL-19 was from R&D Systems (Lille, France).

Construction of an in silico structural model of IL-26

Amino acid sequence analysis, using ClustalW software, showed better identity between IL-26 and IL-10 (26%) compared with IL-19 (20%) and IL-22 (21%). Structural hypothesis of IL-26 was thus built by comparative modeling using the IL-10 x-ray crystal structure as a template for α -parallel bundles. Secondary structure assignments from the amino acid sequence analysis of IL-10 were used to model helices. Virtual 3D construction of the IL-26 model was performed using Modeler software and was validated by Procheck. Electrostatic surface charges were calculated using Adaptive Poisson-Boltzmann Solver (APBS). MetaDBsite was used to determine potential DNA-binding residues. Amphipathic helices were identified using Amphipaseek.

Nucleic acid preparation and NETs isolation

Mammalian genomic DNA was extracted from the human cell line MM6 using a commercial kit (QIAamp DNA kit; Qiagen, Courtaboeuf, France) and partially digested with DNase I (Life Technologies, Saint-Aubin, France); fragmented DNA (200 bp) was purified by ethanol precipitation. Mitochondrial DNA (mtDNA) was amplified by long PCR (primers available upon request) and purified using Agencourt AMPure XP magnetic beads (Beckman Coulter, Villepinte, France). Long mtDNA amplicons were fragmented into 200-bp-long fragments using the IonXpress Plus Fragment Library Kit (Life Technologies). DNA concentration was measured using the Qubit fluorimeter (Life Technologies). NETs were generated by activating neutrophils from healthy donors for 3 h with 100 nM PMA. After washing in PBS, undigested NETs were collected by vigorous pipetting, and cellular debris was removed by centrifugation. Quantification of DNA in NETs was assessed using the PicoGreen dsDNA kit (Life Technologies). Total RNA was isolated from MM6 cells using the RNeasy micro kit (Qiagen). The concentration and purity of nucleic acids were determined by spectrophotometry.

Cell isolation and stimulation

PBMCs were isolated from healthy subjects by standard density-gradient centrifugation on Lymphocyte Separation medium (Eurobio, Courtaboeuf, France). CD14⁺ monocytes were purified from PBMCs by positive magnetic sorting (Miltenyi Biotec, Bergisch Gladbach, Germany). For neutrophil purification, leukocytes were first separated from erythrocytes by density sedimentation with 6% dextran (Sigma-Aldrich, St. Louis, MO), and neutrophils were further isolated from mononuclear cells by density-gradient centrifugation. Purity of monocytes and neutrophils (CD14⁺ and CD66b⁺ cells, respectively) was routinely >95%. CD62L expression was monitored to ensure that neutrophils did not undergo spontaneous activation. Monocytes and neutrophils were cultured in RPMI 1640 medium (Lonza, Verviers, Belgium) supplemented with 10 or 2% FCS (GE Healthcare Life Sciences, Vélizy-Villacoublay, France), respectively, and containing 2 mM glutamine, 1 mM sodium pyruvate, 0.1 mM nonessential amino acids, 10 mM HEPES, and 100 U/ml penicillin and streptomycin (all from Lonza). Neutrophil culture medium was supplemented with 10 μ g/ml heparin (Sigma-Aldrich) and 20 ng/ml GM-CSF (CellGenix, Freiburg, Germany).

IL-26 (50 ng/ml) was incubated or not with 0.1–10 μ g/ml fragmented genomic DNA, 0.01–0.3 μ g/ml NETs, 0.3 μ g/ml mtDNA, or 0.1–10 μ g/ml RNA for 30 min at 37°C before addition to monocytes. As control, monocytes were stimulated with 200 ng/ml LPS (from *E. coli* serotype O111:B4; Sigma-Aldrich). In some experiments, a mix of IL-26 and DNA was treated with 10 IU/ml DNase I before addition to monocytes. In others, cells were treated for 2 h with 50 nM bafilomycin A, 5–20 μ M Z-VAD-FMK, or 10–50 μ M MCC950 (all from Sigma-Aldrich), before addition of DNA plus IL-26.

Human pulmonary artery smooth muscle cells (SMCs) were cultured following manufacturer's instructions (Invitrogen, Carlsbad, CA). Cells were differentiated for 15 d and stimulated or not for 24 h with 100 ng/ml IL-1 β (Miltenyi Biotec) and 100 ng/ml TNF- α (ImmunoTools).

Cytokine quantification

IL-26 was quantified in the sera and cell culture supernatants by ELISA, as previously described (25). IL-1 β , IL-6, and IL-8 were quantified in cell culture supernatants by ELISA (Diacclone, Dijon, France). IL-1 β , IL-6, IL-17, and TNF- α levels were assessed in the sera of AAV patients and healthy subjects using a Bio-Plex ELISA-based immunoassay (Bio-Rad, Hercules, CA).

Detection of circulating IL-26–DNA complexes

IL-26–DNA complexes were assayed in sera by ELISA. In brief, after coating with 5 μ g/ml anti-IL-26 mAb (clone 13C9) and blocking with 1% BSA, plates were incubated with 40 μ l sera before incubation with an HRP-labeled anti-DNA mAb (Roche, Penzberg, Germany). Bound Abs were detected using the peroxidase substrate ABTS (Sigma-Aldrich); results are expressed in OD_{450nm} values.

Analysis of the interaction of IL-26 with nucleic acids

A solid-phase binding assay was performed to analyze the binding of IL-26 to DNA. In brief, 96-well plates (Nunc, Roskilde, Denmark) were coated with 10 μ g/ml DNA or IL-20R1-Fc (R&D Systems), used as positive control (27). After saturation with PBS containing 5% BSA (w/v), plates were successively incubated with 5 μ g/ml IL-26, 0.2 μ g/ml biotinylated anti-IL-26 mAb (clone 8G3), and then with streptavidin-HRP (BD Pharmingen). Bound mAbs were revealed with the 3,3',5,5'-tetramethylbenzidine substrate (Sigma-Aldrich); results are expressed in OD_{450nm} values after subtraction of the values obtained in the absence of IL-26.

Immunohistological analysis

Paraffin-embedded kidney biopsies (Department of Tissue Pathology, University Hospital of Angers) were used to analyze IL-26 expression in kidney biopsies of AAV patients. Slides of normal kidney biopsies from human adults (Biochain, Newark, CA) were used as control. After deparaffinization and Ag demasking, slides were incubated with 10% human serum before incubation with an anti-IL-26 mAb (clone 197505; R&D Systems) or an IgG2b control mAb (BD Biosciences). Bound Abs were detected with a Bond Polymer Refine Detection kit and Peroxidase detection system (both from Leica Microsystems, Newcastle, U.K.). To visualize the IL-26–NETs interaction, we seeded neutrophils on glass coverslips treated with 0.01% poly-L-lysine (Sigma-Aldrich) for 1 h, allowed them to settle, and treated them with 100 nM PMA (Sigma-Aldrich) for 3 h. After fixation with 4% PFA and incubation with 10% mouse serum in PBS, slides were incubated with 5 μ g/ml IL-26 for 1 h. IL-26 was then detected with an anti-IL-26 mAb (clone 197505) labeled with Alexa Fluor 633 (protein labeling kit; Invitrogen) or with an IgG2b control mAb (BD Biosciences). After staining of nuclei with DAPI, slides were mounted in Prolong Gold antifade reagent (Invitrogen) and imaged with a Leica TCS SP8 confocal microscope.

Quantitative RT-PCR analysis

Total RNA extraction and reverse transcription were performed as previously described (23). The expression of IL-1 β , IL-6, IL-26, IFN- β , and STING mRNA was analyzed by quantitative RT-PCR using Maxima SYBR Green qPCR Mastermix (Thermo Scientific); primer sequences are available upon request. Specific gene expression was calculated using the $2^{-\Delta\Delta CT}$ method using GAPDH as calibrator.

Reporter cell lines assay

The involvement of STING was evaluated by using STING-sufficient THP1-Blue IFN-stimulated gene (ISG) cells, which contain an IFN regulatory factor–inducible SEAP reporter construct, and THP1-Blue KD ISG cells, in which the expression of STING is silenced. THP1-Blue ISG and THP1-Blue KD ISG cells, cultured according to the manufacturer's instructions (InvivoGen, Toulouse, France), were stimulated with IL-26, DNA, IL-26–DNA complexes, or 10 μ M 3'3'-cGAMP (InvivoGen); internalization of DNA using the Lipofectamine 2000 transfection reagent (Life Technologies) was used as positive control. SEAP activity was detected using the QUANTI-Blue reporter assay (InvivoGen). Results are expressed as fold induction of reporter activity using PBS-treated samples as reference.

Silencing of TMEM173 expression in monocytes

Short interfering RNA (siRNA) targeting was used to decrease *TMEM173* expression in primary monocytes. Human monocyte nucleofector kit and Nucleofector device were used for delivering siRNA into monocytes,

following the manufacturer's instructions (Lonza). In brief, 8×10^6 monocytes were suspended in 100 μ l of human monocyte nucleofector solution and transfected with ON-TARGETplus siRNA TMEM173 or control siRNA (GE Healthcare Dharmacon, Vélizy-Villacoublay, France) at a final concentration of 100 nM using the Y-001 program. The expression of TMEM173 was assessed by flow cytometry (using AF647-labeled anti-TMEM173 and isotype control mAbs; BD Pharmingen) and by Western blotting using rabbit anti-TMEM173 (R&D Systems) and anti- β -actin (Cell Signaling, Danvers, MA) polyclonal Abs.

Statistical analysis

Data were expressed as mean \pm SEM. Statistical analyses were performed using GraphPad Prism 5 (version 5.02; GraphPad Software, La Jolla, CA). Differences between two groups were assessed using the nonparametric Mann–Whitney *U* test. When analysis included more than two groups, the nonparametric Kruskal–Wallis test or the two-way ANOVA was applied with the Bonferroni–Dunn's posttest comparison. Spearman correlation coefficient was used in univariate analysis. Significant differences are illustrated as **p* < 0.05, ***p* < 0.01, ****p* < 0.001.

Results

IL-26 and extracellular DNA synergize to induce proinflammatory cytokine expression by myeloid cells

To evaluate whether IL-26 may render innate immune cells sensitive to extracellular DNA, we exposed monocytes to 0.1–10 μ g/ml fragmented genomic DNA, either alone or after preincubation with 50 ng/ml IL-26. As previously reported, IL-26 (23), but not extracellular DNA (13), induced IL-6 (Fig. 1A, left panel) and IL-1 β production by monocytes (Fig. 1A, right panel). Interestingly, a preincubation of IL-26 with DNA significantly increased, in a dose-dependent manner, the production of IL-1 β and IL-6 (Fig. 1A). The levels of IL-6 (Fig. 1A) and IL-1 β (data not shown) were not affected when IL-26 plus DNA were treated with DNase I before addition to monocytes. As control, LPS induced IL-1 β and IL-6 production by monocytes (Fig. 1A). IL-6 and IL-1 β mRNA expression were also dramatically enhanced by IL-26 plus DNA, compared with IL-26 alone, but not by DNA alone (Fig. 1B).

This first set of experiments suggested that IL-26 may render DNA stimulatory. DNA sensing induces, in addition to proinflammatory cytokines, the secretion of type I IFNs (1). Accordingly, IL-26 plus DNA upregulated IFN- β mRNA expression by monocytes (Fig. 1B).

The synergistic effect of IL-26 and DNA on proinflammatory cytokine production by monocytes was observed not only with genomic DNA but also with mtDNA (also released by dying cells [36]) and NETs. Whereas NETs alone (used at 10–300 ng/ml NETs-associated DNA content) did not induce detectable IL-6 (Fig. 1A), addition of IL-26 resulted in a huge secretion of IL-6, dependent on the doses of NETs DNA (Fig. 1A). A similar dose-dependent increase of IL-6 production was also observed with IL-26 mixed with RNA (Fig. 1A). None of the other IL-10 family members tested (IL-10, IL-19, IL-22, IL-24, and IL-29) enabled monocytes to sense extracellular DNA (Supplemental Fig. 2).

Myeloid cells are highly sensitive to danger signals. It was thus important to exclude that the activation of monocytes may result from the presence of contaminating molecules. As reported previously (23), IL-26 did not contain stimulatory levels of endotoxins. Moreover, we observed that: 1) the treatment of IL-26 plus DNA with proteinase K abolished their capacity to activate monocytes, and 2) that the treatment of DNA with DNase I or of RNA with RNase before incubation with IL-26 abolished their capacity to potentiate the IL-26–induced secretion of IL-6 by monocytes (data not shown). Collectively, these results suggest that the stimulatory activity of IL-26 and nucleic acids was not associated to the presence of contaminating danger signals.

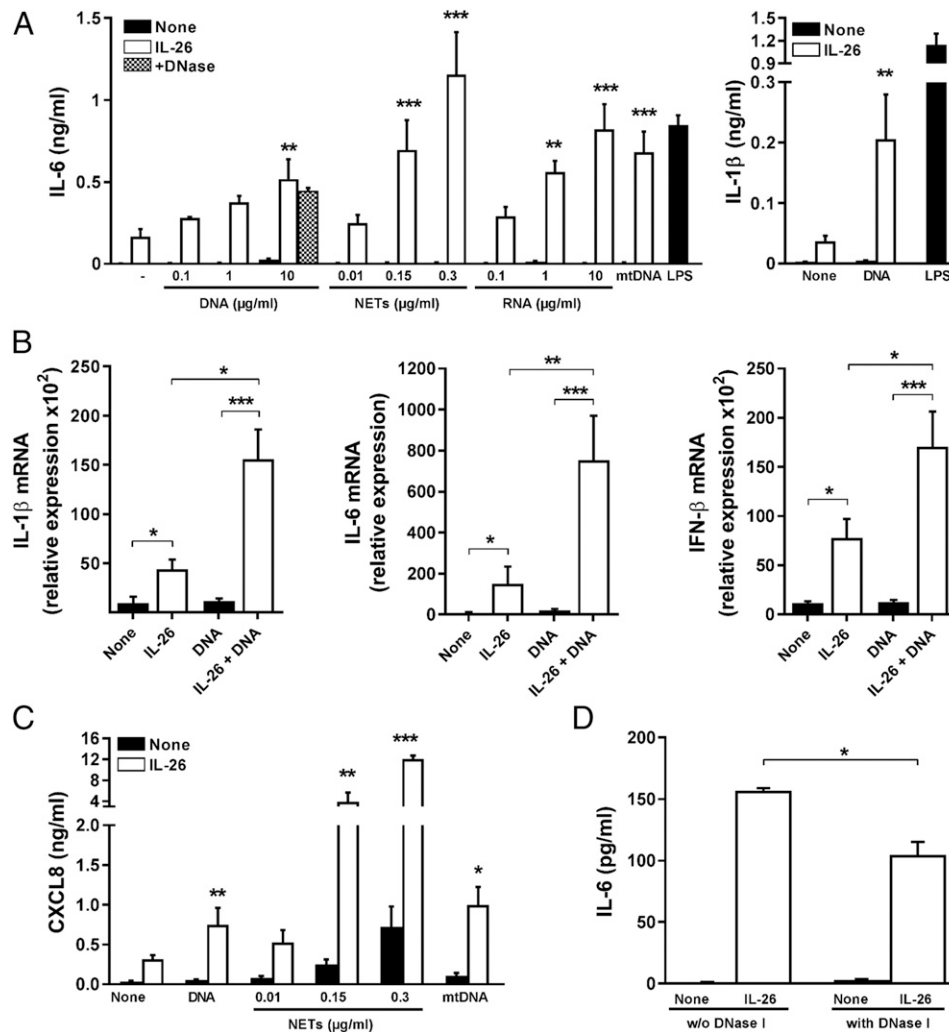


FIGURE 1. IL-26 synergizes with DNA in inducing proinflammatory cytokines and IFN- β expression by myeloid cells. **(A)** Human monocytes were stimulated or not with 50 ng/ml IL-26, in the presence or absence of 0.1–10 μ g/ml genomic DNA, 0.01–0.3 μ g/ml NETs, 0.1–10 μ g/ml RNA, or 0.1 μ g/ml mtDNA. Stimulation with 200 ng/ml LPS was used as a control. IL-6 (left panel) and IL-1 β (right panel) were quantified by ELISA in the 24-h cell culture supernatants. **(B)** Monocytes were stimulated or not for 2 h with 50 ng/ml IL-26 in the presence or absence of 10 μ g/ml genomic DNA. The expression of IL-1 β , IL-6, and IFN- β mRNA was evaluated by quantitative RT-PCR. Results are expressed as a level of mRNA expression relative to GAPDH. **(C)** Human neutrophils were stimulated or not with 50 ng/ml IL-26, in the presence or absence of 10 μ g/ml genomic DNA, 0.01–0.3 μ g/ml NETs, or 0.1 μ g/ml mtDNA. CXCL8 was quantified in the 24-h culture supernatants. **(D)** Monocytes were incubated or not with 10 IU/ml DNase I for 2 h before exposure to 50 ng/ml IL-26. IL-6 was quantified by ELISA in the 24-h culture supernatants. (A–D) Results are expressed as mean \pm SEM of four independent experiments. * p < 0.05, ** p < 0.005, *** p < 0.001. (A, C, and D) Two-way ANOVA with Bonferroni posttest, p value: comparison between IL-26 alone and IL-26 plus DNA. (B) one-way ANOVA.

Neutrophils also became responsive to extracellular DNA in the presence of IL-26. The exposure of neutrophils to IL-26 plus DNA, mtDNA, or NETs induced the production of CXCL8 (Fig. 1C). In contrast, IL-26, as reported previously (37), or DNA alone had a limited effect on CXCL8 secretion by neutrophils (Fig. 1C).

Based on these results, we hypothesized that the ability of IL-26 alone to activate primary myeloid cells (Fig. 1A–C) (23) could result from the presence of nucleic acids released by dying cells during *in vitro* culture. In support, the addition of DNase I into the monocyte cultures before stimulation with IL-26 significantly decreased IL-26-induced IL-6 secretion (Fig. 1D).

As it was detected earlier (as soon as 6 h) and at higher levels than the ones of IL-1 β in response to IL-26 plus nucleic acids, the quantification of IL-6 in cell culture supernatants was used to monitor monocyte activation in the following experiments, unless otherwise stated.

Collectively, these results show that IL-26 synergizes with extracellular self-DNA to induce proinflammatory cytokine secretion by human myeloid cells.

IL-26 exhibits DNA-binding properties

Cell culture assays suggested that IL-26 may interact with nucleic acids. A solid-phase binding assay confirmed that IL-26 bound to immobilized DNA and to IL-20R1, used as a positive control (Fig. 2A). This result was in agreement with the capacity of IL-26 to complex to DNA *in vitro* (26). Immunofluorescence microscopy revealed that IL-26 also bound to the chromatin fibers of NETs (Fig. 2B); no binding of the anti-IL-26 mAb to NETs was observed in the absence of IL-26 (Fig. 2B).

We next explored the structural features of IL-26, which may explain its DNA-binding capacity. In the absence of IL-26 crystal structure, we set up a 3D structural model of IL-26 (Fig. 2C) based on the crystal structure of IL-10, which displays the closest identity with IL-26. This model, generated using the ClustalW

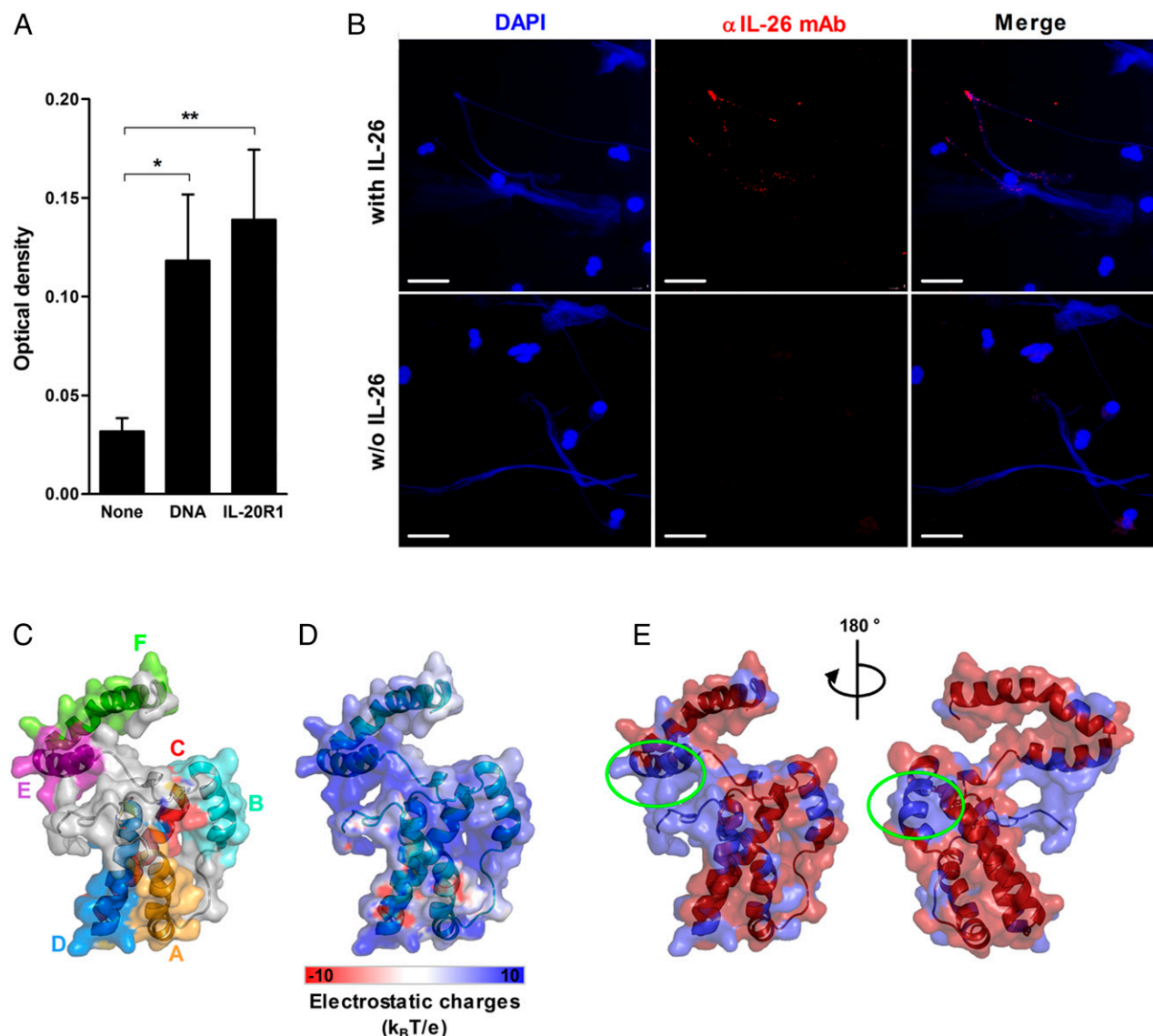


FIGURE 2. IL-26 binds to DNA. **(A)** The binding of IL-26 to immobilized DNA was assessed in a solid-phase binding assay. IL-26 was added to plates coated with 10 $\mu\text{g/ml}$ DNA or IL-20R1-Fc. Bound IL-26 was detected using biotinylated anti-IL-26 mAb revealed with streptavidin-HRP and TMB substrate. Results are expressed in OD_{450nm} values after subtraction of the background (mean \pm SEM, $n = 6$). * $p < 0.05$, ** $p < 0.01$, Mann-Whitney U test. **(B)** NETs were incubated with 5 $\mu\text{g/ml}$ IL-26 (upper panels) or not (lower panels). Bound IL-26 was detected with an Alexa Fluor 633-labeled anti-IL-26 mAb, and DNA was visualized with DAPI. Images are representative of one of two independent experiments. Scale bars, 20 μm . **(C)** A 3D model of IL-26 was generated using the IL-10 x-ray crystal structure as a template and the software Modeler 9v2; this model depicts the six (A–F) α helices. **(D)** Electrostatic potential on the molecular surface of IL-26, calculated using APBS, is colored from red (-10 k_BT/ec) to blue ($+10$ k_BT/ec). **(E)** The blue-colored patches on the molecule surface correspond to DNA-binding domains (green circles), as determined using MetaDBsite.

software and validated using the Procheck software, showed that >90% of residues are located in allowed regions of the Ramachandran plot. Interestingly, analysis with APBS software (38) and with MetaDBsite (39) defined two regions rich in positively charged residues and with predicted DNA-binding properties, composed by helix E and by helix B plus the N terminus of helix C (Fig. 2D, 2E). As observed with the IL-22-based IL-26 model (26), the electrostatic potential on the molecular surface of IL-26 was globally positive.

These results show that IL-26 binds to DNA to form complexes, a property supported by its unconventional cytokine structure.

IL-26 is a cationic amphipathic protein that shuttles extracellular DNA into the cytosol of monocytes

We then investigated whether IL-26 may enable extracellular DNA to access the cytosol of myeloid cells. Monocytes were incubated

with Alexa 488-labeled DNA, in the absence or presence of IL-26, and the percentage of fluorescent monocytes was analyzed by flow cytometry. In the presence of IL-26, an important percentage of fluorescent monocytes was observed; this percentage was dependent on the concentration of DNA (Fig. 3A). Confocal microscopy confirmed the internalization of IL-26–DNA complexes, whereas DNA alone was not internalized (Fig. 3B). Finally, none of the other members of cytokines tested (IL-10, IL-19, IL-22) enabled the internalization of DNA in monocytes (Supplemental Fig. 2).

We then analyzed the biochemical characteristics of IL-26 supporting this property. Among the six α helices (A–F) of IL-26, helices E and F presented amphipathic properties (Fig. 3C), as determined by the Amphipaseek web server. Their helical wheel representations evidenced typical amphipathic α helices with a hydrophobic face and

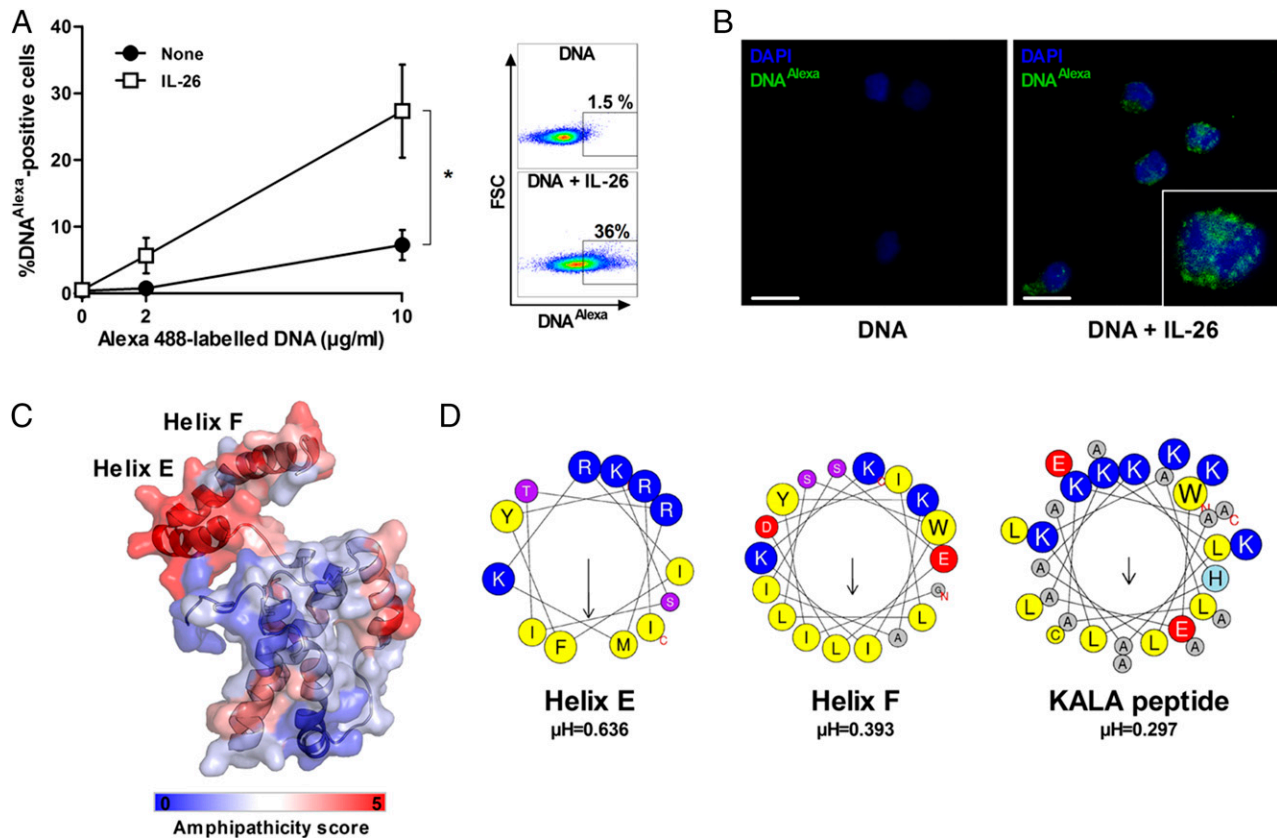


FIGURE 3. IL-26 mediates the internalization of DNA into the cytosol of monocytes. **(A)** The internalization by monocytes of IL-26 complexed with Alexa 488-labeled DNA was assessed by flow cytometry (left panel). Results are expressed as a percentage of fluorescent cells (mean \pm SEM, $n = 7$). Representative dot plots are shown (right panel). $*p < 0.05$, two-way ANOVA. **(B)** The intracellular localization of Alexa 488-labeled DNA within human monocytes after 24-h incubation with or without IL-26 was analyzed by confocal microscopy. Green indicates Alexa 488-labeled DNA; blue indicates DAPI. Scale bars, 10 μm ; insert, higher magnification. **(C)** Surface representation of IL-26 colored according to the amphipathic score, from blue (low) to red (high), using the Amphipathic web server. **(D)** Helical wheel representation of helices E (left panel) and F (middle panel) of IL-26, compared with the CPP KALA (right panel), using HeliQuest (<http://heliquest.ipmc.cnrs.fr/>). The magnitude and direction of the hydrophobic moment (μH) is indicated with a vector arrow.

a hydrophilic face composed of positively charged residues, such as three lysines in helix F (Fig. 3D). DNA-binding domains and amphipathic α helices are features of cationic cell-penetrating peptides (CPPs) designed for DNA delivery, such as the KALA peptide (40). Interestingly, helix F of IL-26 has similarities with the KALA peptide, including an α -helical conformation with a hydrophilic face including lysine residues and a hydrophobic face including leucine residues (Fig. 3D). Finally, helix F was also predicted to have an in-plane membrane (IPM) motif anchor, involved in the binding of proteins to cell membranes (41).

Collectively, these results show that IL-26 displays features of CPPs (large positive area, two amphipathic helices, and an IPM anchor), which may contribute to explaining its capacity to shuttle DNA within myeloid cells.

The activation of monocytes by IL-26–DNA complexes involves STING and the inflammasome

We next investigated by which mechanism IL-26–DNA complexes activate monocytes. Previous studies reported that the inflammasome-dependent production of IL-1 β by DNA-stimulated myeloid cells involves caspase 1 and NLRP3 (42, 43), and that IL-1 β can induce the autocrine production of IL-6 (44). Accordingly, the production of IL-6 induced by IL-26–DNA complexes was reduced in the presence of the pan-caspase inhibitor Z-VAD-FMK (90.4 \pm 4.3% inhibition with 20 μM Z-VAD-FMK; mean \pm

SEM, $n = 4$) and of the NLRP3 inhibitor MCC950 (57.4 \pm 8.1% inhibition with 50 μM MCC950) (Fig. 4A).

However, IL-26–DNA complexes also induce, in addition to proinflammatory cytokines, the expression of IFN- β , whose production is not dependent on inflammasome activation (45). We thus hypothesized that IL-26–DNA complexes may stimulate myeloid cells via DNA sensors and focused on those that induce both IFN- β and proinflammatory cytokines synthesis, namely TLR9 and STING. In agreement with the fact that TLR9 is absent in human monocytes (46), bafilomycin A, a specific blocker of endosomal TLR signaling (47), did not reduce monocyte (Fig. 4B, left panel) and neutrophil (Fig. 4B, right panel) activation by IL-26–DNA complexes. As control, bafilomycin A prevented the activation of monocytes and neutrophils by the endosomal TLR7/8 ligand CL097 (Fig. 4B).

STING was reported to be involved in DNA-induced inflammatory cytokine production by human myeloid cells (13, 48). We first compared the response of the cell line THP1-ISG, either or not silenced for STING (THP1-ISG-KD STING and THP1-ISG, respectively), with IL-26–DNA complexes. Results showed that, contrary to THP1-ISG cells, THP1-ISG-KD STING cells did not respond to IL-26–DNA complexes (Fig. 4C). As expected, THP1-ISG-KD STING cells were also less sensitive to the STING ligand 3'3'-cGAMP and to transfected DNA, compared with THP1-ISG cells (Fig. 4C). Second, silencing STING using siRNA significantly decreased the production of IL-26 by monocytes in response

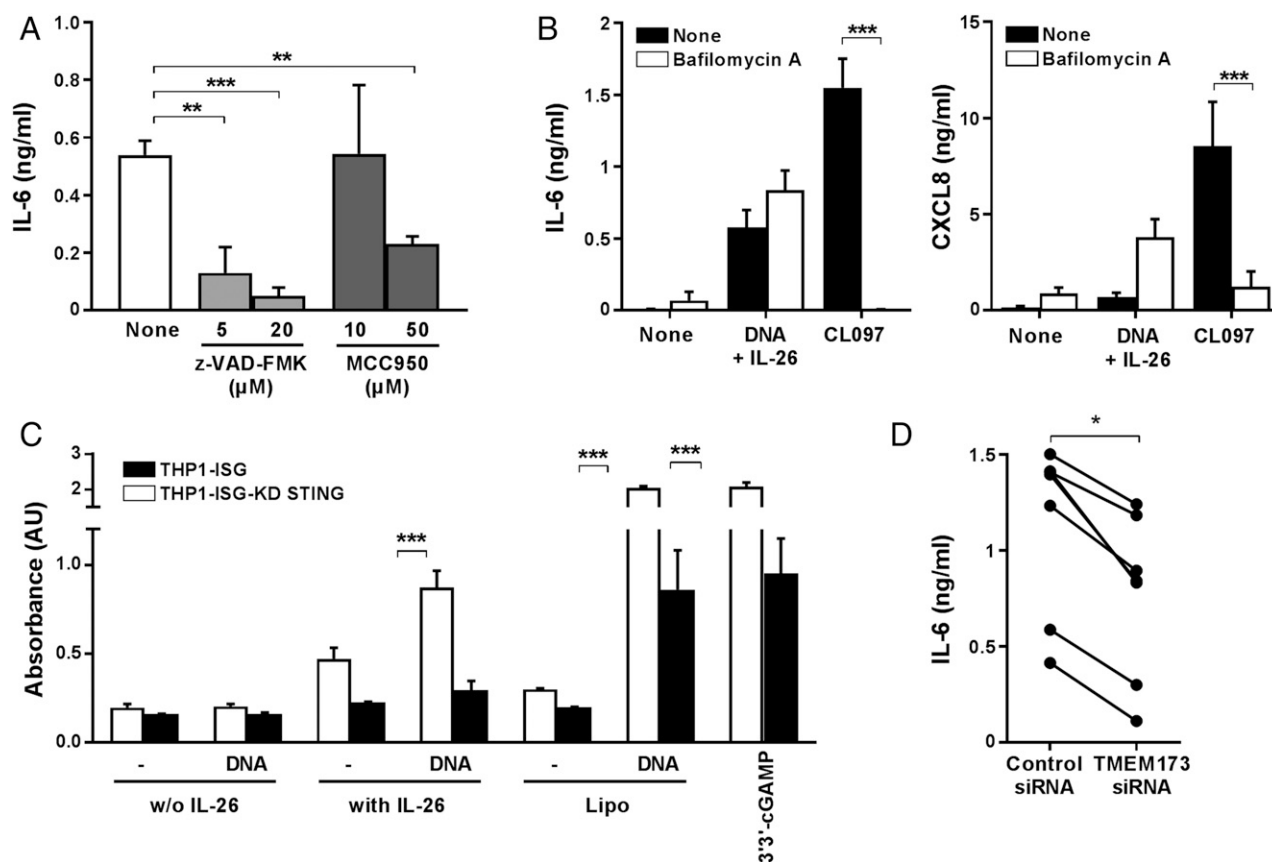


FIGURE 4. The activation of monocytes with IL-26–DNA complexes is dependent on inflammasome and STING activation. **(A)** Human monocytes were stimulated with 50 ng/ml IL-26 in the presence of 10 μ g/ml DNA without or with 5–20 μ M Z-VAD-FMK or 10–50 μ M MCC950. IL-6 was quantified in the 24-h cell culture supernatants by ELISA. **(B)** Monocytes (left panel) or neutrophils (right panel) were incubated or not with 50 nM bafilomycin A for 2 h before exposure to 50 ng/ml IL-26 plus 10 μ g/ml genomic DNA, or to 250 ng/ml CL097, a synthetic TLR7/8 agonist. IL-6 and CXCL8 were quantified by ELISA in the 24-h culture supernatants. **(C)** The human myeloid cell line THP1-ISC, either knocked down or not for STING (THP1-ISC-KD STING and THP1-ISC, respectively), used at 5×10^5 cells/ml, was stimulated for 24 h with 400 ng/ml IL-26, 10 μ g/ml DNA, 400 ng/ml IL-26 plus 10 μ g/ml DNA, or 10 μ M 3'-cGAMP (a synthetic STING agonist), or was transfected with 10 μ g/ml genomic DNA using the Lipofectamine 2000 reagent (Lipo). ISG5A promoter activity was measured by a chromogenic (SEAP substrate) assay. **(D)** Monocytes were transfected for 48 h with siRNA targeting TMEM173 (STING) mRNA or control siRNA before stimulation with 50 ng/ml IL-26 plus 10 μ g/ml genomic DNA. IL-6 was quantified in the 24-h cell culture supernatants by ELISA. Results are expressed as mean \pm SEM of six independent experiments (* p < 0.05, Wilcoxon test). (A–C) Data are shown as mean \pm SEM of four independent experiments. * p < 0.05, ** p < 0.01, *** p < 0.001. (A) one-way ANOVA; (B and C) two-way ANOVA.

to IL-26–DNA complexes, compared with control siRNA (Fig. 4D). As control, siRNA targeting STING decreased STING mRNA expression and protein expression, as assessed by flow cytometry ($24.8 \pm 4.0\%$ decrease of MFI value; mean \pm SEM, $n = 6$) and Western blotting (Supplemental Fig. 3); STING expression was not modulated in monocytes transfected with control siRNA (Supplemental Fig. 3). Finally, we observed that IL-26–DNA complexes and IL-26 induced the phosphorylation of IFN regulatory factor 3 (Supplemental Fig. 3), which is involved in the signaling pathway downstream of STING.

These results demonstrate that IL-26 renders extracellular DNA able to signal via the inflammasome and the cytosolic STING pathway, a result in line with the capacity of IL-26 to shuttle extracellular DNA into myeloid cells.

In AAV patients with crescentic glomerulonephritis, vascular SMCs of renal arteries express IL-26

We have shown that IL-26 plus DNA induce proinflammatory cytokines via STING. A constitutive activation of STING in STING-associated vasculopathy with onset in infancy patients results in unabated systemic inflammation and vasculitis (49). AAV is a chronic and remitting autoimmune disease that targets microvessel walls and is associated with: 1) a systemic and local

inflammation (50), 2) a massive cell death in injured tissues associated with elevated serum levels of nucleosomes (51), and 3) a type I IFN signature (elevated seric circulating type I IFN levels and tissue MxA expression in active AAV) (52). This last point suggests a break in innate immune tolerance to self-DNA. We thereby hypothesized that IL-26 could be present and involved, together with DNA released by dying cells, in AAV.

We first analyzed by immunochemistry the expression of IL-26 in kidney biopsies of active AAV patients. Kidney is one of the main target organs in AAV, with glomerulonephritis characterized by crescentic necrotizing lesions (53). Biopsies of active patients revealed an intense staining with an anti-IL-26 mAb of vascular SMCs from arteries (Fig. 5A) and from afferent glomerular arterioles (data not shown), whereas endothelial cells and fibroblasts were not stained (Fig. 5A). No staining of vascular SMCs was observed with a control mAb. Kidney arteries and afferent glomerular arterioles from healthy subjects were not stained by the anti-IL-26 mAb (Fig. 5A).

Confirming that SMCs may represent a novel source of IL-26, we observed that cultured human primary SMCs constitutively expressed IL-26 mRNA (Fig. 5B); moreover, intracellular IL-26 was detected by immunofluorescence in nonstimulated cells

FIGURE 5. IL-26 expression in vascular SMCs in the kidney of patients with AAV glomerulonephritis. **(A)** The expression of IL-26 was evaluated by immunohistochemistry in kidney biopsies from AAV patients or healthy subjects. Slides were incubated with an anti-IL-26 mAb or an isotype control mAb; bound Abs were detected with a Bond Polymer Refine Detection kit and peroxidase detection system. (Left) Staining with anti-IL-26 mAb; (right) staining with the isotype control mAb. Scale bars, 50 μ m. **(B)** IL-26 mRNA expression was analyzed by quantitative RT-PCR in differentiated vascular SMCs, stimulated or not for 24 h with 100 ng/ml IL-1 β and 100 ng/ml TNF- α ; results are expressed as the level of mRNA expression relative to GAPDH. **(C)** The expression of IL-26 by differentiated vascular SMCs stimulated or not for 24 h with 100 ng/ml IL-1 β and 100 ng/ml TNF- α was analyzed by immunofluorescence, using Alexa Fluor 633-labeled anti-IL-26 mAb. Scale bars, 100 μ m. Results are representative of one out of three independent experiments. **(D)** Quantification by ELISA of IL-26 in the supernatants of differentiated vascular SMCs stimulated for 24 h with 100 ng/ml IL-1 β and 100 ng/ml TNF- α . **(E)** The expression of IL-26 was evaluated by immunohistochemistry in kidney biopsies from AAV patients with crescentic glomerulonephritis (as in A). (Left panels) Staining with anti-IL-26 mAb; (right panels) staining with isotype control mAb. Scale bars, 50 μ m. (B and C) Data are shown as mean \pm SEM ($n = 3$). * $p < 0.05$, Mann-Whitney U test. (A and E) Results are representative of one of four independent experiments.

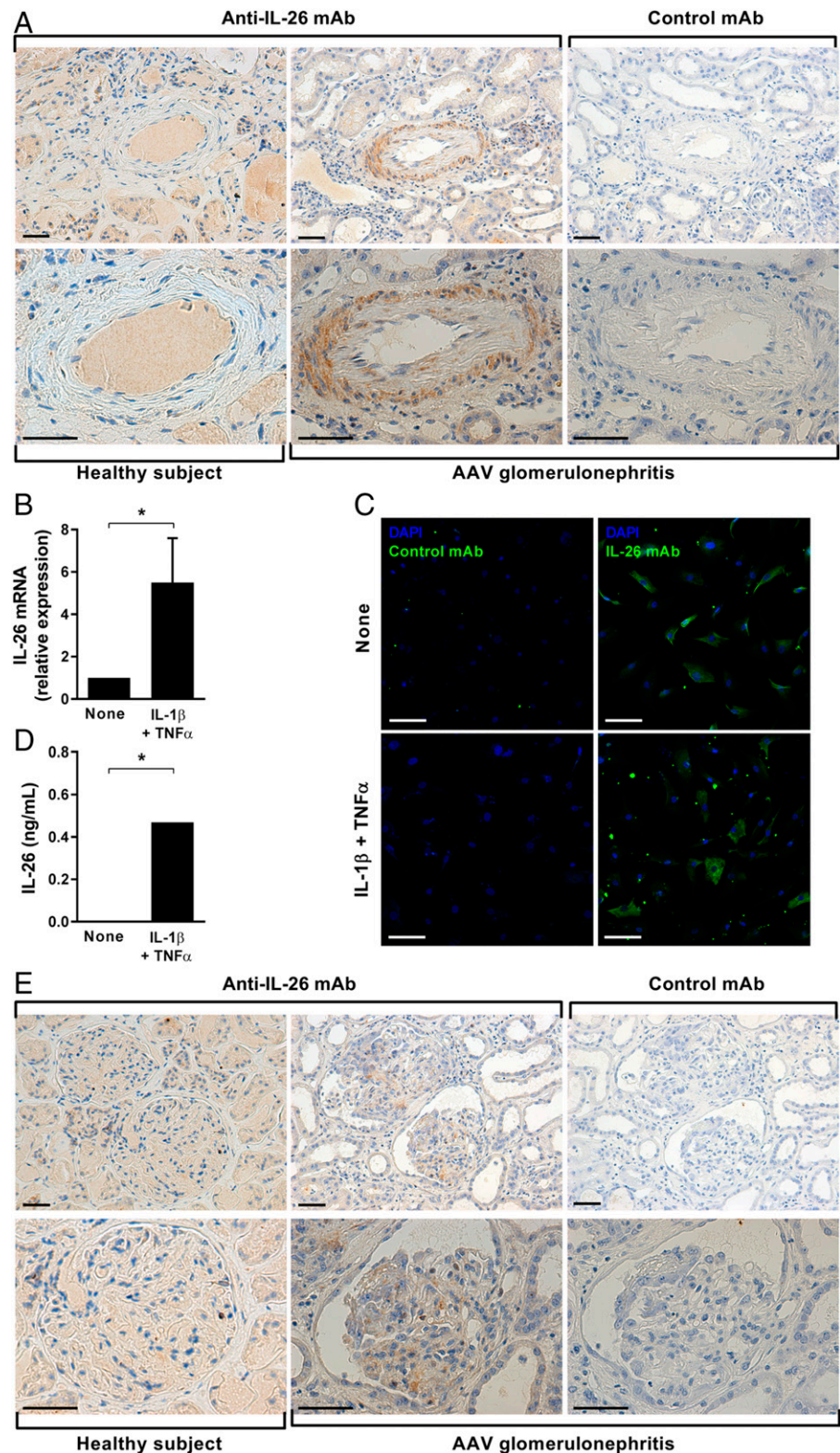


(Fig. 5C). Stimulation of SMCs with the proinflammatory cytokines IL-1 β and TNF- α upregulated IL-26 mRNA expression (Fig. 5B) and IL-26 production (Fig. 5C, 5D). Finally, IL-26 expression by arterial SMCs was associated with a diffuse IL-26 labeling in crescentic glomeruli (Fig. 5E); glomeruli from healthy subjects were not stained by anti-IL-26 mAb (Fig. 5E).

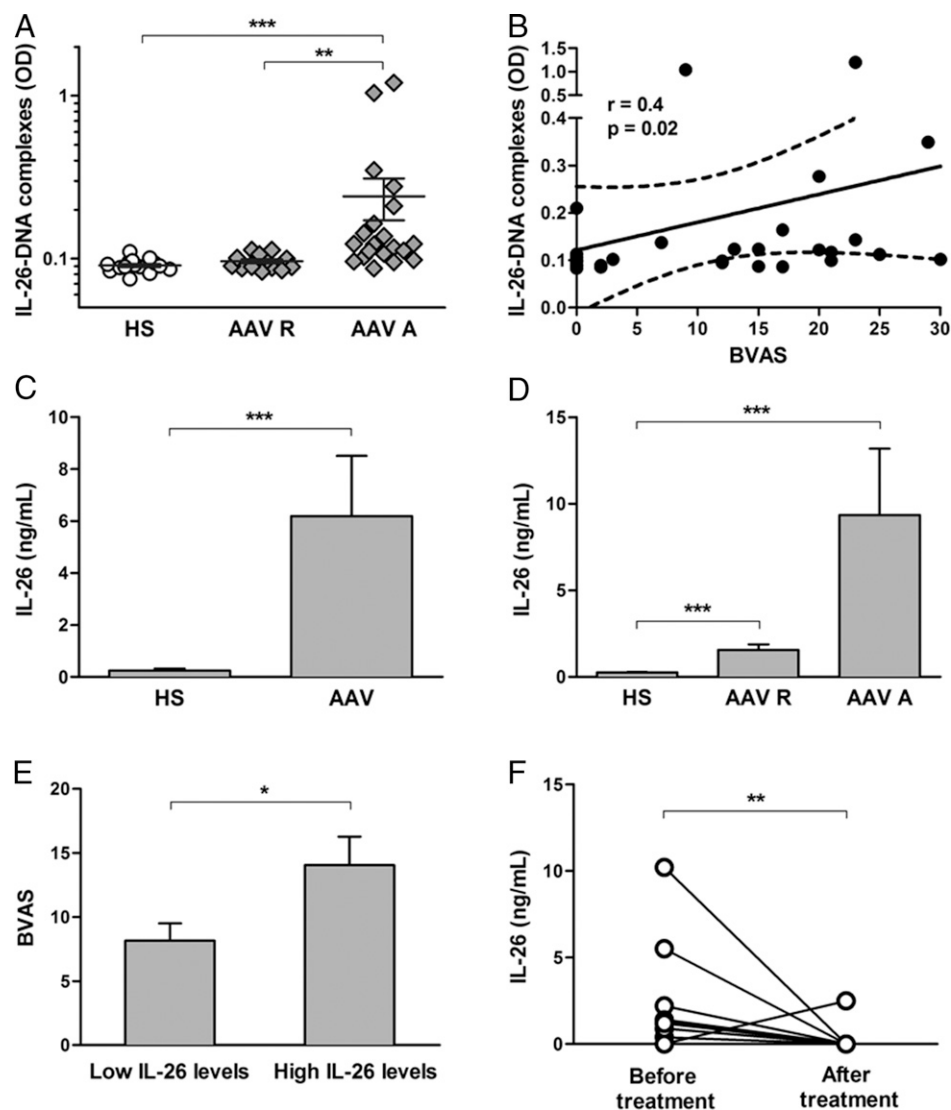
These results show that, in active AAV patients, IL-26 is produced by renal arterial SMCs and is present in crescentic glomeruli,

lesions characterized by massive cell infiltration and cell death (leukocytoclasia) (53).

IL-26–DNA complexes and high levels of IL-26 are detected in the sera of active AAV patients

The expression of IL-26 by arterial SMCs suggested the systemic presence of IL-26. Because circulating DNA is present in active AAV patients (51), we hypothesized that IL-26–DNA complexes

FIGURE 6. Analysis of IL-26 and IL-26–DNA complexes in AAV patients. **(A)** IL-26–DNA complexes were assessed by ELISA in the sera of AAV patients ($n = 35$; acute disease: AAV A, $n = 20$; remission disease: AAV R, $n = 15$) and healthy subjects (HS) ($n = 16$). **(B)** Circulating IL-26–DNA complexes were correlated to BVAS in AAV patients ($n = 32$) (Spearman correlation coefficient). **(C)** IL-26 was quantified by ELISA in the sera of healthy subjects (HS) ($n = 85$) and AAV patients ($n = 69$). **(D)** IL-26 levels were analyzed according to disease activity status: AAV patients in remission (AAV R; $n = 28$) and AAV patients with active disease (AAV A; $n = 41$). **(E)** BVAS value according to serum IL-26 levels (low: <2.4 ng/ml, $n = 45$; high: >2.4 ng/ml, $n = 24$). The cutoff value of IL-26 was determined as the mean value + 2 SD determined in healthy subjects. **(F)** IL-26 was quantified in the sera of 10 AAV patients at the disease onset and 6–12 mo of follow-up. (A and C–E) Data are shown as mean \pm SEM. * $p < 0.05$, ** $p < 0.005$, *** $p < 0.001$. (A and D) Kruskal–Wallis test; (C) t test; (E and F) Mann–Whitney U test.



may exist in vivo. Interestingly, we evidenced the presence of circulating IL-26–DNA complexes by ELISA in 11 of 20 active AAV patients (Fig. 6A), with levels that positively correlated with BVAS ($r = 0.4$, $p = 0.02$) (Fig. 6B). In contrast, these complexes remained undetectable in remitting AAV patients and healthy subjects (Fig. 6A). The concentrations of serum IL-26 were higher in AAV patients ($n = 69$) than in healthy subjects ($n = 85$) (6.2 ng/ml [0–140] versus 0.25 ng/ml [0–4.7], respectively) (Fig. 6C). Both active and remitted patients exhibited a higher concentration of IL-26 (9.3 ng/ml [0–140] and 1.6 ng/ml [0–8], respectively) than healthy subjects (Fig. 6D). The ELISA used in this study quantifies total IL-26 (complexed or not to DNA; data not shown). Although IL-26 levels were not statistically higher in active than in remitted patients, those with high IL-26 concentration (>2.4 ng/ml, corresponding to mean + 2 SD of IL-26 level determined in healthy subjects) had a higher BVAS than patients with low IL-26 concentration (≤ 2.4 ng/ml) (8.2 ± 9.2 and 14 ± 10.9 , respectively) (Fig. 6E). Interestingly, 9 of 10 patients, for whom blood samples were available at flare-up and 6–12 mo after the initiation of an immunosuppressive treatment, exhibited a decrease in circulating IL-26 after treatment (Fig. 6F).

In conclusion, active AAV patients exhibit IL-26 in necrotic lesions and circulating IL-26–DNA complexes (Fig. 7).

Discussion

IL-26 is a member of the IL-10 cytokine subfamily overexpressed in different chronic inflammatory diseases (e.g., Crohn's disease, rheumatoid arthritis, psoriasis, chronic hepatitis C virus infection, and graft-versus-host disease) for which biological activity remains unclear (23–26, 54). We report in this article that IL-26: 1) exhibits several features of CPPs designed for DNA transfection and, 2) allows myeloid cells to be activated by extracellular DNA in an inflammasome-dependent and STING-dependent manner. In support of these observations, AAV patients with glomerulonephritis display IL-26 deposits in injured kidneys and circulating IL-26–DNA complexes. IL-26 thus appears as a proinflammatory molecule that links extensive cell death and sustained inflammation.

We demonstrate in this study that IL-26 shuttles extracellular DNA into the cytosol of human myeloid cells. This property is supported by its unique biochemical and structural features (cationicity and amphipathicity), which are similar to the ones of cell-penetrating (40) and antimicrobial peptides (55), such as the cathelicidin LL-37 (13, 14). In this study, we propose an IL-26 structural model based on IL-10 because IL-10 displays the closest identity with IL-26 and both cytokines have an alkaline isoelectric point. The overall high cationic charge of IL-26 supports its DNA-binding properties; more precisely, we identify the helices B and E as the main DNA-binding motifs in IL-26. Moreover, the IL-10-based

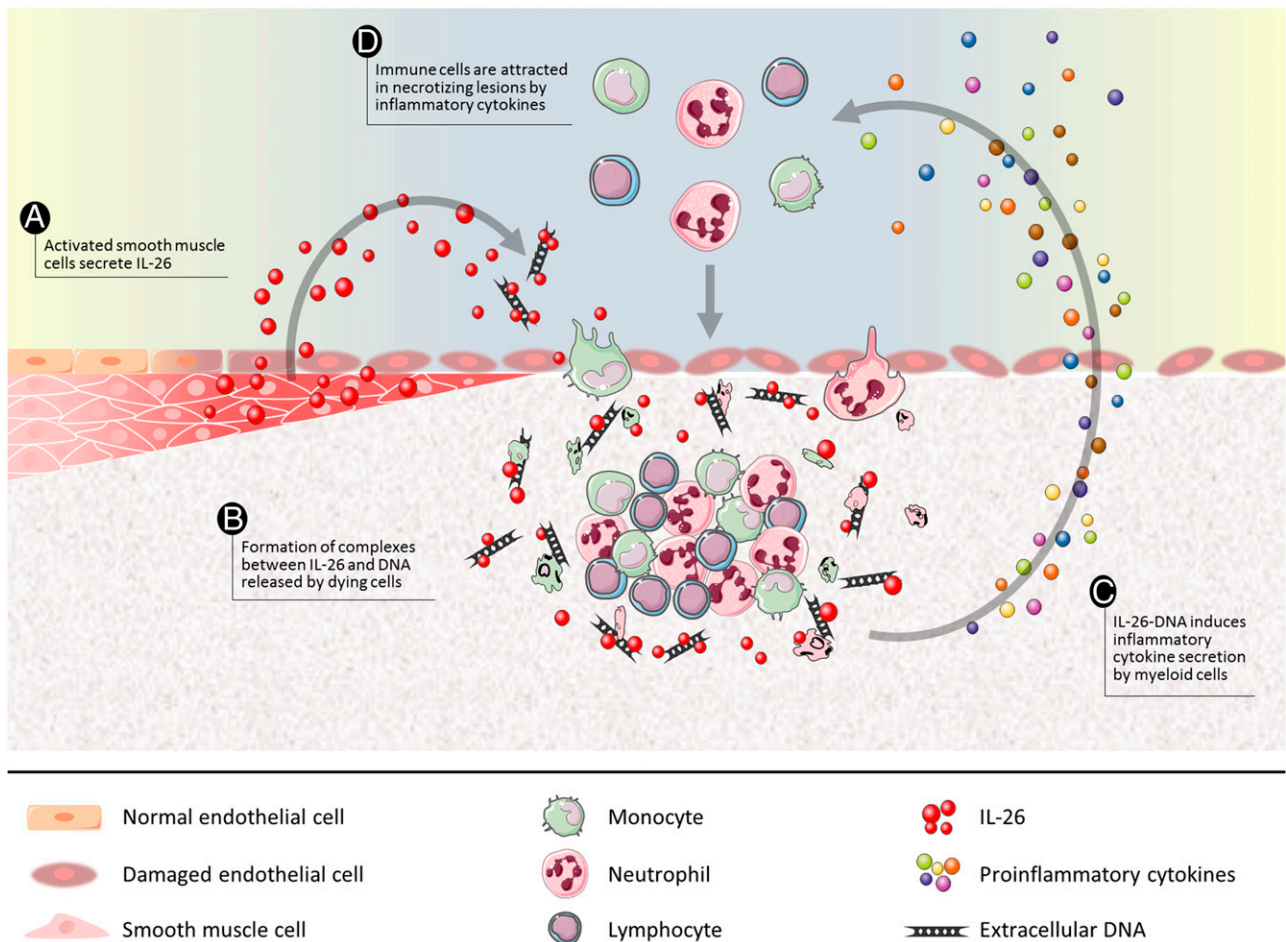


FIGURE 7. Schematic representation of the role of IL-26 in active AAV. Vascular kidney SMCs of patients with crescentic necrotizing lesions produce IL-26 (**A**). As a consequence of its unique cationic and amphipathic properties, IL-26 binds to self-DNA released by dying cells (**B**). IL-26 sustains the inflammatory process by enabling myeloid cells to sense dying cell DNA (**C**), thereby establishing a harmful positive amplification loop that may potentiate the inflammation process (recruitment of neutrophils, production of IL-26-induced cytokines in necrotizing lesions) (**D**). This scheme was drawn using modified pictures from [Servier Medical Art](#) under a [Creative Commons Attribution 3.0 Unported License](#).

model predicts that the amphipathic helix F displays an accessible IPM anchor. IPM anchors are present in several proteins, especially antimicrobial and CPPs, and allow their insertion at the membrane interfaces. In support, although IL-10 and IL-19 are also fairly cationic (pHi 8 and pHi 7.6, respectively) and display amphipathic helices, IL-26 is the only one to enable monocytes to sense DNA.

In accordance with our findings, a recent study, using an IL-22-based model, showed that IL-26 exhibits some structural features of antimicrobial peptides (26). Contrary to IL-10, IL-22 has a global neutral charge (pHi 7.1). Overall, the IL-10- and IL-22-based models exhibit similarities, including the preservation of disulphide bonds and amphipathicity, but also differences. The IL-22-based model predicts that IL-26 may adopt a beads-on-string shape, supportive of its direct antimicrobial activity (26). However, contrary to the IL-10-based model, this model does not predict an accessible IPM anchor. Of note, the N terminus of IL-26, which may act as a noncovalent intermolecular linker to form multimeric IL-26, remains accessible in the IL-10-based IL-26 model. In accordance with our model, the IL-22-based model also suggested that IL-26 aggregates and condensates DNA to form insoluble particles that can be internalized by target cells.

IL-26 thus combines: 1) a high cationic charge, 2) the proximity of two amphipathic α helices with an accessible IPM anchor, and 3) the capacity to shuttle extracellular DNA into myeloid cells. IL-26

thus appears as a unique endogenous DNA transfection protein with structural and biochemical properties similar to CPPs.

In agreement with our previous study reporting that IL-26 is proinflammatory (23), our results showed that IL-26–DNA complexes induce the production of IL-6 and IL-1 β by human monocytes. Interestingly, IL-1 β , whose secretion requires inflammasome activation, can induce, in an autocrine manner, the secretion of IL-6 (44). Accordingly, the production of IL-6 by monocytes stimulated with IL-26–DNA complexes was reduced upon inhibition of caspases and NLRP3. However, the fact that IL-26–DNA complexes also induced type I IFNs, the production of which is not dependent on NLRP3 or AIM-2 inflammasomes (56), was in favor of the involvement of an intracellular DNA sensor (such as STING or IFI16), whose engagement can also induce inflammatory cytokines (1). In agreement with this hypothesis, results showed that the activation of human myeloid cells by IL-26–DNA complexes also involved STING, a cytosolic adapter that can be activated directly by DNA or by upstream DNA sensors, mainly cGAS (57). In support of this, and in agreement with others (48), the STING ligand 3'3'-cGAMP induced, in addition to IFN- β , the expression of IL-1 β and IL-6 by human monocytes (data not shown). Collectively, our results show that the activation of human monocytes by IL-26–DNA complexes involves STING and the inflammasome, most probably caspases, although the relative roles of these pathways cannot be determined.

IL-26 confers immunostimulatory properties to the different types of DNA (i.e., genomic DNA, mtDNA, and NETs). Previous studies have evidenced that genomic and mtDNA, released upon cell injury (36), activate the STING pathway (4, 58, 59). NETs have been reported in AAV and SLE and are suspected to contribute to breaking innate tolerance to self-DNA (60, 61). Notably, in the presence of IL-26, myeloid cells are strongly activated by low concentrations of NETs, suggesting a major proinflammatory role of IL-26 at sites of neutrophil accumulation and death. Because STING expression is not restricted to myeloid cells (2), it remains to be evaluated whether other STING-expressing human cell types respond to IL-26 plus DNA.

Previous in vitro studies have shown that IL-26 stimulates proinflammatory cytokine secretion by monocytes (23) and NK (25) cells, in the absence of IL-20R1 expression. In line with these observations, DNase I significantly prevents IL-26-induced activation, showing that the activation induced by IL-26 alone is partly mediated by DNA released by dying cells in culture.

The observation that DNase I does not totally inhibit in vitro the effect of IL-26 on monocytes could be explained by the ability of IL-26 to protect extracellular DNA from DNase I (26), or to protect cytosolic self-DNA from intracellular DNases, leading to a cytosolic DNA accumulation that activates STING (6, 62, 63).

In contrast with human myeloid cells, pDCs express functional TLR9 and respond to IL-26 plus DNA via TLR9 (26). Surprisingly, this activation required ~700-fold higher levels of IL-26 than IL-26 plus DNA-induced myeloid cell activation, suggesting that IL-26–DNA complexes preferentially activate myeloid cells.

Finally, the use of transgenic IL-26 mice to assess in vivo the role of IL-26 in DNA-induced inflammation is precluded because murine myeloid cells are not sensitive to human IL-26 plus DNA (data not shown). In parallel, murine myeloid cells do not sense DNA–CPP (LL37 or KALA) complexes, whereas they are responsive to the STING activator 3′3′-cGAMP (data not shown). The efficiency of CPP on murine cells has hitherto not been reported and seems to be cell lineage (64–66) and species dependent (67).

Collectively, these data show that IL-26 acts as a self-DNA cargo molecule that triggers proinflammatory cytokine secretion by human myeloid cells.

In line with these results, we were interested in AAV patients, especially during acute flare-ups. Indeed, the acute lesions begin as a neutrophil-rich necrotizing inflammation, with admixed monocytes producing destructive necrotizing vascular and extravascular inflammation (53). We show in this study that active AAV patients exhibit high levels of circulating IL-26 and, interestingly, of IL-26–DNA complexes. Immunohistochemistry revealed that vascular SMCs from kidney biopsies of active AAV patients express IL-26. Moreover, we observed that, in vitro, a combination of IL-1 β and TNF- α , which are overexpressed in vasculitis (68), induce IL-26 expression by differentiated vascular SMCs. We provide evidence in this article of activated SMCs as an IL-26–producing cell type. In line with this observation, SMCs are known to produce proinflammatory cytokines and to participate in immune cell extravasation (69). This result does not exclude that Th17 cells, which are present in AAV lesions (68), may also contribute to IL-26 expression. In conclusion, in active AAV lesions, IL-26 seems produced locally, especially by vascular SMCs, and accumulates in necrotizing crescentic lesions, characterized by accumulation of dead cells and leukocytoclasia. IL-26 may therefore contribute to boost local proinflammatory cytokine secretion, thereby amplifying not only cell recruitment and death but also IL-26 secretion, as a positive feedback loop (Fig. 7). It would be of interest to assess IL-26 implication in the pathophysiology of other chronic inflammatory disorders

associated with cell death, sustained inflammation, and an overexpression of IL-26, such as rheumatoid arthritis and Crohn's disease (23–26).

In conclusion, IL-26 appears as a unique cationic and amphipathic protein, more similar to a soluble pattern recognition receptor than to a conventional cytokine, that links dying cell DNA and uncontrolled inflammation. IL-26 thereby constitutes a promising target to dampen sustained inflammation.

Acknowledgments

We thank members of the cellular and molecular (PACeM) and microscopy (SCIAM) facilities of the University of Angers and members of the histopathology laboratory of the University Hospital of Angers for expert technical assistance.

Disclosures

The authors have no financial conflicts of interest.

References

- Paludan, S. R. 2015. Activation and regulation of DNA-driven immune responses. *Microbiol. Mol. Biol. Rev.* 79: 225–241.
- Ishikawa, H., and G. N. Barber. 2008. STING is an endoplasmic reticulum adaptor that facilitates innate immune signalling. *Nature* 455: 674–678.
- Barber, G. N. 2015. STING: infection, inflammation and cancer. *Nat. Rev. Immunol.* 15: 760–770.
- Ishikawa, H., Z. Ma, and G. N. Barber. 2009. STING regulates intracellular DNA-mediated, type I interferon-dependent innate immunity. *Nature* 461: 788–792.
- Napirei, M., H. Karsunky, B. Zevnik, H. Stephan, H. G. Mannherz, and T. Mörröy. 2000. Features of systemic lupus erythematosus in Dnase1-deficient mice. *Nat. Genet.* 25: 177–181.
- Stetson, D. B., J. S. Ko, T. Heidmann, and R. Medzhitov. 2008. Trex1 prevents cell-intrinsic initiation of autoimmunity. *Cell* 134: 587–598.
- Yoshida, H., Y. Okabe, K. Kawane, H. Fukuyama, and S. Nagata. 2005. Lethal anemia caused by interferon-beta produced in mouse embryos carrying undigested DNA. *Nat. Immunol.* 6: 49–56.
- Demaria, O., J. Di Domizio, and M. Gilliet. 2014. Immune sensing of nucleic acids in inflammatory skin diseases. *Semin. Immunopathol.* 36: 519–529.
- Kawane, K., M. Ohtani, K. Miwa, T. Kizawa, Y. Kanbara, Y. Yoshioka, H. Yoshikawa, and S. Nagata. 2006. Chronic polyarthritis caused by mammalian DNA that escapes from degradation in macrophages. *Nature* 443: 998–1002.
- Ahn, J., D. Gutman, S. Saijo, and G. N. Barber. 2012. STING manifests self DNA-dependent inflammatory disease. *Proc. Natl. Acad. Sci. USA* 109: 19386–19391.
- Yang, Y. G., T. Lindahl, and D. E. Barnes. 2007. Trex1 exonuclease degrades ssDNA to prevent chronic checkpoint activation and autoimmune disease. *Cell* 131: 873–886.
- Barton, G. M., J. C. Kagan, and R. Medzhitov. 2006. Intracellular localization of Toll-like receptor 9 prevents recognition of self DNA but facilitates access to viral DNA. *Nat. Immunol.* 7: 49–56.
- Chamilos, G., J. Gregorio, S. Meller, R. Lande, D. P. Kontoyiannis, R. L. Modlin, and M. Gilliet. 2012. Cytosolic sensing of extracellular self-DNA transported into monocytes by the antimicrobial peptide LL37. *Blood* 120: 3699–3707.
- Lande, R., J. Gregorio, V. Facchinetti, B. Chatterjee, Y. H. Wang, B. Homey, W. Cao, Y. H. Wang, B. Su, F. O. Nestle, et al. 2007. Plasmacytoid dendritic cells sense self-DNA coupled with antimicrobial peptide. *Nature* 449: 564–569.
- Yasuda, K., P. Yu, C. J. Kirschning, B. Schlatter, F. Schmitz, A. Heit, S. Bauer, H. Hochrein, and H. Wagner. 2005. Endosomal translocation of vertebrate DNA activates dendritic cells via TLR9-dependent and -independent pathways. *J. Immunol.* 174: 6129–6136.
- Schauer, C., C. Janko, L. E. Munoz, Y. Zhao, D. Kienhöfer, B. Frey, M. Lell, B. Manger, J. Rech, E. Naschberger, et al. 2014. Aggregated neutrophil extracellular traps limit inflammation by degrading cytokines and chemokines. *Nat. Med.* 20: 511–517.
- Means, T. K., E. Latz, F. Hayashi, M. R. Murali, D. T. Golenbock, and A. D. Luster. 2005. Human lupus autoantibody–DNA complexes activate DCs through cooperation of CD32 and TLR9. *J. Clin. Invest.* 115: 407–417.
- Garcia-Romo, G. S., S. Caielli, B. Vega, J. Connolly, F. Allantaz, Z. Xu, M. Punaro, J. Baisch, C. Guiducci, R. L. Coffman, et al. 2011. Netting neutrophils are major inducers of type I IFN production in pediatric systemic lupus erythematosus. *Sci. Transl. Med.* 3: 73ra20.
- Wolk, K., S. Kunz, K. Asadullah, and R. Sabat. 2002. Cutting edge: immune cells as sources and targets of the IL-10 family members? *J. Immunol.* 168: 5397–5402.
- Trivella, D. B., J. R. Ferreira-Júnior, L. Dumoutier, J. C. Renauld, and I. Polikarpov. 2010. Structure and function of interleukin-22 and other members of the interleukin-10 family. *Cell. Mol. Life Sci.* 67: 2909–2935.

21. Donnelly, R. P., F. Sheikh, H. Dickensheets, R. Savan, H. A. Young, and M. R. Walter. 2010. Interleukin-26: an IL-10-related cytokine produced by Th17 cells. *Cytokine Growth Factor Rev.* 21: 393–401.
22. Braum, O., H. Pirzer, and H. Fickenscher. 2012. Interleukin-26, a highly cationic T-cell cytokine targeting epithelial cells. *Antinflamm. Antiallergy Agents Med. Chem.* 11: 221–229.
23. Corvaisier, M., Y. Delneste, H. Jeanvoine, L. Preisser, S. Blanchard, E. Garo, E. Hoppe, B. Barré, M. Audran, B. Bouvard, et al. 2012. IL-26 is overexpressed in rheumatoid arthritis and induces proinflammatory cytokine production and Th17 cell generation. *PLoS Biol.* 10: e1001395.
24. Dambacher, J., F. Beigel, K. Zitzmann, E. N. De Toni, B. Göke, H. M. Diepolder, C. J. Auernhammer, and S. Brand. 2009. The role of the novel Th17 cytokine IL-26 in intestinal inflammation. *Gut* 58: 1207–1217.
25. Miot, C., E. Beaumont, D. Duluc, H. Le Guillou-Guillemette, L. Preisser, E. Garo, S. Blanchard, I. Hubert Fouchard, C. Crémion, P. Lamourette, et al. 2015. IL-26 is overexpressed in chronically HCV-infected patients and enhances TRAIL-mediated cytotoxicity and interferon production by human NK cells. *Gut* 64: 1466–1475.
26. Meller, S., J. Di Domizio, K. S. Voo, H. C. Friedrich, G. Chamilos, D. Ganguly, C. Conrad, J. Gregorio, D. Le Roy, T. Roger, et al. 2015. T(H)17 cells promote microbial killing and innate immune sensing of DNA via interleukin 26. *Nat. Immunol.* 16: 970–979.
27. Hör, S., H. Pirzer, L. Dumoutier, F. Bauer, S. Wittmann, H. Sticht, J. C. Renaud, R. de Waal Malefyt, and H. Fickenscher. 2004. The T-cell lymphokine interleukin-26 targets epithelial cells through the interleukin-20 receptor 1 and interleukin-10 receptor 2 chains. *J. Biol. Chem.* 279: 33343–33351.
28. Sheikh, F., V. V. Baurin, A. Lewis-Antes, N. K. Shah, S. V. Smirnov, S. Anantha, H. Dickensheets, L. Dumoutier, J. C. Renaud, A. Zdanov, et al. 2004. Cutting edge: IL-26 signals through a novel receptor complex composed of IL-20 receptor 1 and IL-10 receptor 2. *J. Immunol.* 172: 2006–2010.
29. Nagalakshmi, M. L., E. Murphy, T. McClanahan, and R. de Waal Malefyt. 2004. Expression patterns of IL-10 ligand and receptor gene families provide leads for biological characterization. *Int. Immunopharmacol.* 4: 577–592.
30. Wolk, K., K. Witte, E. Witte, S. Proesch, G. Schulze-Tanzil, K. Nasilowska, J. Thilo, K. Asadullah, W. Sterry, H. D. Volk, and R. Sabat. 2008. Maturing dendritic cells are an important source of IL-29 and IL-20 that may cooperatively increase the innate immunity of keratinocytes. *J. Leukoc. Biol.* 83: 1181–1193.
31. Shi, C., and E. G. Pamer. 2011. Monocyte recruitment during infection and inflammation. *Nat. Rev. Immunol.* 11: 762–774.
32. Kolaczowska, E., and P. Kubes. 2013. Neutrophil recruitment and function in health and inflammation. *Nat. Rev. Immunol.* 13: 159–175.
33. Stone, J. H., G. S. Hoffman, P. A. Merkel, Y. I. Min, M. L. Uhlfelder, D. B. Hellmann, U. Specks, N. B. Allen, J. C. Davis, R. F. Spiera, et al.; International Network for the Study of the Systemic Vasculitides (INSSYS). 2001. A disease-specific activity index for Wegener's granulomatosis: modification of the Birmingham Vasculitis Activity Score. *Arthritis Rheum.* 44: 912–920.
34. Mukhtyar, C., L. Guillevin, M. C. Cid, B. Dasgupta, K. de Groot, W. Gross, T. Hauser, B. Hellmich, D. Jayne, C. G. Kallenberg, et al.; European Vasculitis Study Group. 2009. EULAR recommendations for the management of primary small and medium vessel vasculitis. *Ann. Rheum. Dis.* 68: 310–317.
35. Knappe, A., S. Hör, S. Wittmann, and H. Fickenscher. 2000. Induction of a novel cellular homolog of interleukin-10, AK155, by transformation of T lymphocytes with herpesvirus saimiri. *J. Virol.* 74: 3881–3887.
36. Zhang, Q., M. Raouf, Y. Chen, Y. Sumi, T. Sursal, W. Junger, K. Brohi, K. Itagaki, and C. J. Hauser. 2010. Circulating mitochondrial DAMPs cause inflammatory responses to injury. *Nature* 464: 104–107.
37. Che, K. F., S. Tengvall, B. Levänen, E. Silverpil, M. E. Smith, M. Awad, M. Vikström, L. Palmberg, I. Qvarfordt, M. Sköld, and A. Lindén. 2014. Interleukin-26 in antibacterial host defense of human lungs. Effects on neutrophil mobilization. *Am. J. Respir. Crit. Care Med.* 190: 1022–1031.
38. Baker, N. A., D. Sept, S. Joseph, M. J. Holst, and J. A. McCammon. 2001. Electrostatics of nanosystems: application to microtubules and the ribosome. *Proc. Natl. Acad. Sci. USA* 98: 10037–10041.
39. Si, J., Z. Zhang, B. Lin, M. Schroeder, and B. Huang. 2011. MetaDBSite: a meta approach to improve protein DNA-binding sites prediction. *BMC Syst. Biol.* 5 (Suppl. 1): S7.
40. Copolovici, D. M., K. Langel, E. Eriste, and Ü. Langel. 2014. Cell-penetrating peptides: design, synthesis, and applications. *ACS Nano* 8: 1972–1994.
41. Sapay, N., Y. Guernneur, and G. Deléage. 2006. Prediction of amphipathic in-plane membrane anchors in monotopic proteins using a SVM classifier. *BMC Bioinformatics* 7: 255.
42. Coward, W. R., A. Marei, A. Yang, M. M. Vasa-Nicotera, and S. C. Chow. 2006. Statin-induced proinflammatory response in mitogen-activated peripheral blood mononuclear cells through the activation of caspase-1 and IL-18 secretion in monocytes. *J. Immunol.* 176: 5284–5292.
43. Shin, M. S., Y. Kang, N. Lee, E. R. Wahl, S. H. Kim, K. S. Kang, R. Lazova, and I. Kang. 2013. Self double-stranded (ds)DNA induces IL-1 β production from human monocytes by activating NLRP3 inflammasome in the presence of anti-dsDNA antibodies. *J. Immunol.* 190: 1407–1415.
44. Tosato, G., and K. D. Jones. 1990. Interleukin-1 induces interleukin-6 production in peripheral blood monocytes. *Blood* 75: 1305–1310.
45. Hornung, V., A. Ablasser, M. Charrel-Dennis, F. Bauernfeind, G. Horvath, D. R. Caffrey, E. Latz, and K. A. Fitzgerald. 2009. AIM2 recognizes cytosolic dsDNA and forms a caspase-1-activating inflammasome with ASC. *Nature* 458: 514–518.
46. Hornung, V., S. Rothenfusser, S. Britsch, A. Krug, B. Jahrsdörfer, T. Giese, S. Endres, and G. Hartmann. 2002. Quantitative expression of toll-like receptor 1-10 mRNA in cellular subsets of human peripheral blood mononuclear cells and sensitivity to CpG oligodeoxynucleotides. *J. Immunol.* 168: 4531–4537.
47. Lund, J., A. Sato, S. Akira, R. Medzhitov, and A. Iwasaki. 2003. Toll-like receptor 9-mediated recognition of Herpes simplex virus-2 by plasmacytoid dendritic cells. *J. Exp. Med.* 198: 513–520.
48. Ahn, J., P. Ruiz, and G. N. Barber. 2014. Intrinsic self-DNA triggers inflammatory disease dependent on STING. *J. Immunol.* 193: 4634–4642.
49. Liu, Y., A. A. Jesus, B. Marrero, D. Yang, S. E. Ramsey, G. A. Montealegre Sanchez, K. Tenbrock, H. Wittkowski, O. Y. Jones, H. S. Kuehn, et al. 2014. Activated STING in a vascular and pulmonary syndrome. *N. Engl. J. Med.* 371: 507–518.
50. Ohlsson, S., J. Wieslander, and M. Segelmark. 2004. Circulating cytokine profile in anti-neutrophilic cytoplasmic autoantibody-associated vasculitis: prediction of outcome? *Mediators Inflamm.* 13: 275–283.
51. Holdenrieder, S., P. Eichhorn, U. Beuers, W. Samtleben, U. Schoenmarck, R. Zachoval, D. Nagel, and P. Stieber. 2006. Nucleosomal DNA fragments in autoimmune diseases. *Ann. N. Y. Acad. Sci.* 1075: 318–327.
52. Kessenbrock, K., M. Krumbholz, U. Schönemarch, W. Back, W. L. Gross, Z. Werb, H. J. Gröne, V. Brinkmann, and D. E. Jenne. 2009. Netting neutrophils in autoimmune small-vessel vasculitis. *Nat. Med.* 15: 623–625.
53. Jenette, J. C., and R. J. Falk. 2014. Pathogenesis of antineutrophil cytoplasmic autoantibody-mediated disease. *Nat. Rev. Rheumatol.* 10: 463–473.
54. Ohnuma, K., R. Hatano, T. M. Aune, H. Otsuka, S. Iwata, N. H. Dang, T. Yamada, and C. Morimoto. 2015. Regulation of pulmonary graft-versus-host disease by IL-26+CD26+CD4 T lymphocytes. *J. Immunol.* 194: 3697–3712.
55. Zasloff, M. 2002. Antimicrobial peptides of multicellular organisms. *Nature* 415: 389–395.
56. Gray, E. E., D. Winship, J. M. Snyder, S. J. Child, A. P. Geballe, and D. B. Stetson. 2016. The AIM2-like receptors are dispensable for the interferon response to intracellular DNA. *Immunity* 45: 255–266.
57. Paludan, S. R., and A. G. Bowie. 2013. Immune sensing of DNA. *Immunity* 38: 870–880.
58. White, M. J., K. McArthur, D. Metcalf, R. M. Lane, J. C. Cambier, M. J. Herold, M. F. van Delft, S. Bedoui, G. Lessene, M. E. Ritchie, et al. 2014. Apoptotic caspases suppress mtDNA-induced STING-mediated type I IFN production. *Cell* 159: 1549–1562.
59. Rongvaux, A., R. Jackson, C. C. Harman, T. Li, A. P. West, M. R. de Zoete, Y. Wu, B. Yordy, S. A. Lakhani, C. Y. Kuan, et al. 2014. Apoptotic caspases prevent the induction of type I interferons by mitochondrial DNA. *Cell* 159: 1563–1577.
60. Lande, R., D. Ganguly, V. Facchinetti, L. Frasca, C. Conrad, J. Gregorio, S. Meller, G. Chamilos, R. Sebasigari, V. Ricciari, et al. 2011. Neutrophils activate plasmacytoid dendritic cells by releasing self-DNA-peptide complexes in systemic lupus erythematosus. *Sci. Transl. Med.* 3: 73ra19.
61. Knight, J. S., W. Zhao, W. Luo, V. Subramanian, A. A. O'Dell, S. Yalavarthi, J. B. Hodgins, D. T. Eitzman, P. R. Thompson, and M. J. Kaplan. 2013. Peptidylarginine deiminase inhibition is immunomodulatory and vasculoprotective in murine lupus. *J. Clin. Invest.* 123: 2981–2993.
62. Härtlova, A., S. F. Ertmann, F. A. Raffi, A. M. Schmalz, U. Resch, S. Anugula, S. Lienenklaus, L. M. Nilsson, A. Kröger, J. A. Nilsson, et al. 2015. DNA damage primes the type I interferon system via the cytosolic DNA sensor STING to promote anti-microbial innate immunity. *Immunity* 42: 332–343.
63. Volkman, H. E., and D. B. Stetson. 2014. The enemy within: endogenous retroelements and autoimmune disease. *Nat. Immunol.* 15: 415–422.
64. Hurtado, P., and C. A. Peh. 2010. LL-37 promotes rapid sensing of CpG oligodeoxynucleotides by B lymphocytes and plasmacytoid dendritic cells. *J. Immunol.* 184: 1425–1435.
65. Hasan, M., C. Ruksznis, Y. Wang, and C. A. Leifer. 2011. Antimicrobial peptides inhibit polyinosinic-polycytidylic acid-induced immune responses. *J. Immunol.* 187: 5653–5659.
66. Merkle, M., J. Pircher, H. Mannell, F. Krötz, P. Blüm, T. Czernak, E. Gaitzsch, C. Schneider, S. Köppel, A. Ribeiro, and M. Wörnle. 2015. LL37 inhibits the inflammatory endothelial response induced by viral or endogenous DNA. *J. Autoimmun.* 65: 19–29.
67. Nakagawa, Y., and R. L. Gallo. 2015. Endogenous intracellular cathelicidin enhances TLR9 activation in dendritic cells and macrophages. *J. Immunol.* 194: 1274–1284.
68. Nogueira, E., S. Hamour, D. Sawant, S. Henderson, N. Mansfield, K. M. Chavele, C. D. Pusey, and A. D. Salama. 2010. Serum IL-17 and IL-23 levels and autoantigen-specific Th17 cells are elevated in patients with ANCA-associated vasculitis. *Nephrol. Dial. Transplant.* 25: 2209–2217.
69. Lacolley, P., V. Regnault, A. Nicoletti, Z. Li, and J. B. Michel. 2012. The vascular smooth muscle cell in arterial pathology: a cell that can take on multiple roles. *Cardiovasc. Res.* 95: 194–204.